Preparation and Characterization of Multi-Walled Carbon Nanotube/Poly(ethylene terephthalate) Nanoweb

Byung Wook Ahn, Yong Seung Chi, Tae Jin Kang

Department of Materials Science and Engineering, Seoul National University, Sillim-dong, Gwanak-gu, Seoul 151-742, Korea

Received 22 February 2008; accepted 21 July 2008
DOI 10.1002/app.28968
Published online 23 September 2008 in Wiley InterScience (www.interscience.wiley.com).

ABSTRACT: Multi-walled carbon nanotube (MWCNT)/Poly(ethylene terephthalate) (PET) nanowebs were obtained by electrospinning. For uniform dispersion of MWCNTs in PET solution, MWCNTs were functionalized by acid treatment. Introduction of carboxyl groups onto the surface of MWCNTs was examined by Fourier transform infrared (FTIR) spectroscopy and X-ray diffraction (XRD) analysis. MWCNTs were added into 22 wt % PET solution in the ratio of 1, 2, 3 wt % to PET. The morphology of MWCNT/PET nanoweb was observed using field emission-scanning electron microscopy (FE-SEM) and transmission electron microscopy (TEM). The nanofiber diameter decreased with increasing MWCNT concentration. The distribution of the nanofiber diameters showed a bi-modal shape when MWCNTs were added. Thermal and tensile properties of electrospun MWCNT/PET nanowebs were examined using a differential scanning calorimeter (DSC), thermogravimetric analyzer (TGA), dynamic mechanical analyzer (DMA) and etc. Tensile strength, tensile modulus, thermal stability, and the degree of crystallinity increased with increasing MWCNT concentration. In contrast, elongation at break and cold crystallization temperature showed a contrary tendency. Electric conductivities of the MWCNT/PET nanowebs were in the electrostatic dissipation range. © 2008 Wiley Periodicals, Inc. J Appl Polym Sci 110: 4055–4063, 2008

Key words: nanocomposites; polyesters; electron microscopy; mechanical properties; thermal properties

INTRODUCTION

Carbon nanotube (CNT) has attracted much interest due to its excellent mechanical and electrical properties since it was first discovered by Ijima in 1991.[1] For single-walled carbon nanotube (SWCNT), tensile modulus is known to be about 1 TPa[2] and electrical conductivity comes up to 10^3 times higher than copper. But it seems that multi-walled carbon nanotube (MWCNT) gathers more interest due to its easy processability and low cost in spite of inferior properties to SWCNT. Among the broad applications of CNT,[3–5] many attempts have been made for CNT/polymer blend including nanocomposites,[6,7] films,[8,9] electrospun nanowebs.[10,11] Although preserving the intrinsic properties of the polymer, remarkable improvement in various properties could be achieved by the addition of a small amount of CNT. However, CNTs easily tend to aggregate with each other due to Van der Waals force.[12] Consequently, uniform dispersion in polymer matrix is difficult and property enhancement by CNT addition is severely depreciated due to aggregations. Several methods including polymer wrapping, surfactant treatment, and chemical modification[13–15] have been tried to obtain uniform dispersion.

As the diameter of fibers decreases from submicrons to nanometers, the surface area/volume ratio of fiber increases by geometric progression. There are several methods to obtain micro- or nano-fibers. Commonly used methods include template synthesis,[16] phase separation,[17] self-assembly,[18] electrospinning,[19,20] etc. Electrospinning is an easy method to produce nanofibers using simple equipment. Recently, electrospinning with two and more materials has been used to obtain nanowebs which have excellent mechanical or electrical properties with large surface area/volume ratio.[21–23] Especially, it has been documented that electrospinning method is capable of aligning CNTs along the fiber axis by charge, confinement and flow effect.[24]

Since Poly(ethylene terephthalate) (PET) is a important commercial thermoplastic polymer, several works about preparation and characterization of CNT/PET composites were done. The works were confined to composite films,[9] nanocomposites by melt-compounding,[25] and conventional fibers by blend-spinning,[26] mainly. However, studies on CNT/PET nanowebs are still not done in spite of

Correspondence to: T. J. Kang (taekang@snu.ac.kr).
Contract grant sponsor: Korea Science and Engineering Foundation (KOSEF; through the SRC/ERC program of MOST/KOSEF); contract grant number: R11-2005-065.

Journal of Applied Polymer Science, Vol. 110, 4055–4063 (2008)

the potentialities in various applications. In this work, we functionalized MWCNTs by acid treatment to introduce carboxyl groups onto the MWCNT surface and fabricated electrospun nanowebs using functionalized MWCNTs and PET. Functionalization of MWCNTs was examined and the morphology of the electrospun MWCNT/PET nanoweb was observed. Tensile, thermal, and electrical properties of the MWCNT/PET nanowebs were also examined.

EXPERIMENTAL

Materials and preparation of electrospinning dope

MWCNTs (CM-95, >95%) were purchased from Iljin nanotech, Korea. Poly(ethylene terephthalate) (PET, M_w 19,200) bright chips were supplied by Toray-Saehan, Korea.

The MWCNTs were treated with sulfuric acid to achieve good uniform dispersion of MWCNTs in the organic solvent. MWCNTs were leached in 3*M* H_2SO_4 with mild stirring at 90°C for 3 h. By sulfuric acid treatment, the residual catalysts and metal oxides were removed. Then, the mixture was filtered through a glass filter and washed with distilled water. After drying in a vacuum oven for 24 h, MWCNTs were oxidized with 98% H_2SO_4 at 90°C for 2 h. This process was necessary to remove the amorphous carbon layer and introduce carboxyl groups onto the surface of MWCNTs. Glass filtering, washing with distilled water and drying in a vacuum oven were followed.

The purified MWCNTs were added into Trifluoro acetic acid (TFA, 99%) and the mixture was bath-sonicated for 30 min. PET chips were added little by little into the MWCNT/TFA mixture with bath-sonicating. PET concentration was always 22 wt % in TFA. In this way, MWCNT/PET dopes were prepared with MWCNT concentrations of 1, 2, and 3 wt % to PET. For comparison, neat PET solution was also prepared by dissolving PET chips into TFA by magnetic stirring.

Electrospinning

The morphology of electrospun nanowebs can be controlled by several electrospinning parameters and dope concentration. To obtain uniform and even shaped nanofibers, the following electrospinning conditions were used. These optimized conditions are based on previous experimental results done in our lab.

The prepared dope was electrospun using a high voltage supplier (CPS-40K03, Chungpa EMT, South Korea). The applied voltage was fixed to 15 kV, and tip-to-collector distance was 15 cm. The inner diameter of the metal syringe tip was 19 gauge (0.686 mm). To obtain nanowebs of even thickness, an aluminum drum able of traversing and rotating movement was used as the collector. The rotating velocity was 600 rpm and the traversing velocity was 5 cm/s. Electrospinning dope was pushed out using a syringe pump (No. 200, KdScientific, USA) at a rate of 2 mL/h. The syringe tip was located in the horizontal direction of the collector. For even thickness of nanoweb samples, 2 g of PET was electrospun in all cases. The electrospun nanowebs were dried in the vacuum oven for 3 days to completely evaporate TFA.

Characterization

Introduction of carboxyl groups on the surface of MWCNT was examined using a Fourier transform infrared spectrometer (FTIR Spectrum 2000, Perkin–Elmer, Waltham, MA). Removal of the residual metal from MWCNT was examined using an X-ray diffraction analyzer (Nanostar small-angle X-ray scattering system, Bruker, Germany) with Cu K_α radiation. The change in dope viscosity with the shear rate was examined at 25°C using a rheometer (Physica MCR 301, Anton Paar, Austria). The rheometer was run with 20-mm parallel-plate geometry and 0.68-mm sample gap. The morphology of electrospun nanowebs was observed with a field emission-scanning electron microscope (FE-SEM JSM-6330F, JEOL, Japan). The distribution of nanofiber diameters was measured using a built-in counting program. High resolution transmission electron microscope (HR-TEM JEM-3010, JEOL) was utilized to observe the size and alignment of MWCNTs in PET nanofiber with an accelerating voltage of 300 kV.

Calorimetric measurements were performed using a differential scanning calorimeter (DSC 823e, Mettler Toledo, Columbus, OH). The samples were heated from 40 to 300°C at a heating rate of 10°C/min under nitrogen atmosphere. The degree of crystallinity was calculated to examine the changes in crystallinity caused by MWCNT addition. The degree of crystallinity was calculated by the following equation:

$$\chi = \frac{\Delta H_f - \Delta H_c}{(1 - M_{\mathrm{CNT}})\Delta H_f^{\mathrm{o}}} \times 100\%$$

where, χ is the degree of crystallinity of MWCNT/PET nanoweb, M_{CNT} is the concentration of MWCNT, ΔH_f is the measured heat of melting, ΔH_c is the measured heat of cold crystallization, ΔH_f^{o} is the heat of fusion of 100% crystalline PET. ΔH_f^{o} was set as 105.97 J/g.[27] Thermal stability of samples was measured using a thermogravimetric analyzer (TGA 7, Perkin–Elmer). The samples were heated from 30 to 600°C at a heating rate of 5°C/min under nitrogen atmosphere.

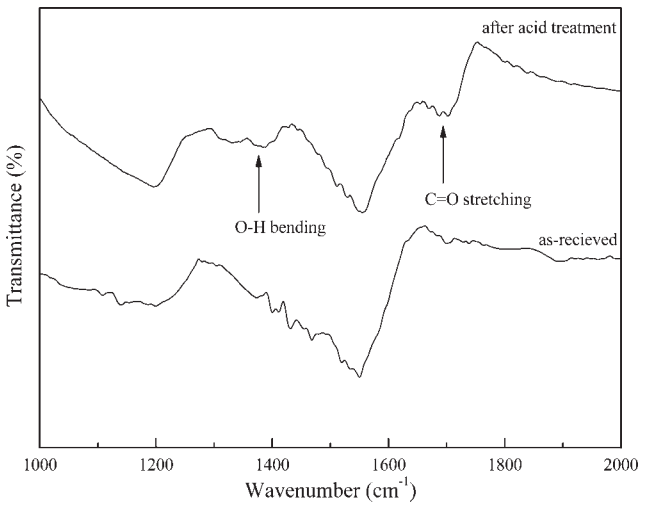

Figure 1 FTIR spectra of MWCNTs before and after acid treatment.

Tensile properties were tested using an universal testing machine (MMT2000, Rheometric Scientific Inc., Piscataway, NJ). The specimens for tensile properties were tested in the direction of collector rotation. Dynamic mechanical analysis (DMA) was also carried out using an dynamic mechanical thermal analyzer (DMTA V, Rheometric Science) under air atmosphere from 40 to 100°C at a heating rate of 5°C/min. The samples were tested by tension mode with a static strain of 0.1 and a vibration frequency of 1 Hz. All mechanical tests were performed with sample size of 20 mm (gap) × 10 mm (width) × ~ 0.25 mm (thickness).

The electrical conductivity was measured using the 4-point probe method, with a digital source meter (2400, Keithley, Cleveland, OH) at room temperature. The electrical conductivity was calculated using the following equation.[28]

$$\sigma(\mathrm{S/cm}) = \frac{l}{dw}\frac{I}{V}$$

where, l (cm) is the gap between electrodes, d (cm) is the thickness of web, w (cm) is the length of electrode, I (A) is the current applied to the nanoweb, and V (V) is the measured voltage.

RESULTS AND DISCUSSION

Morphology

Figure 1 shows the FTIR spectra of as-received and acid treated MWCNTs. The peaks at ca 1550 cm^{-1} and ca 1200 cm^{-1} are typical peaks of CNT assigned to the carbon skeleton.[29] The introduction of carboxyl groups was confirmed by the two peaks. One at 1730 cm^{-1} is associated with C=O stretching of carboxyl acids and the other at 1400 cm^{-1} is associated with O—H bending of carboxyl acids and phenolic groups.[29] The dispersion of the functionalized MWCNTs in TFA looks stable by the hydrogen bonding between TFA and the carboxyl groups attached to the MWCNT surface as shown in Figure 2.

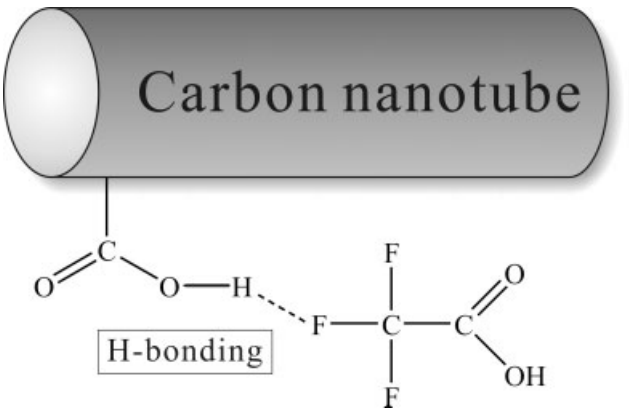

Figure 2 A diagram of the interaction model of TFA and functionalized MWCNT.

The XRD spectra of MWCNTs before and after acid treatment are given in Figure 3. In both spectra, two peaks appeared at 25.8° and 43° corresponding to the diffraction of the (002) and (100) crystal planes of MWCNTs.[30] The disappearance of the α-Fe peak at 50.3° after acid treatment confirmed the removal of residual metal catalysts and metal oxides.[31]

Figure 4 shows the SEM photographs of MWCNT/PET nanowebs. The average diameter of nanofibers decreased as the MWCNT concentration increased. CNTs could act as charge carriers, increasing the Coulomb force acted on the electrospinning dope. As the attractive force between the electrospinning jet and the collector increases, the nanofibers experience a higher stretching force.[32] It is well-known that increase in dope viscosity causes

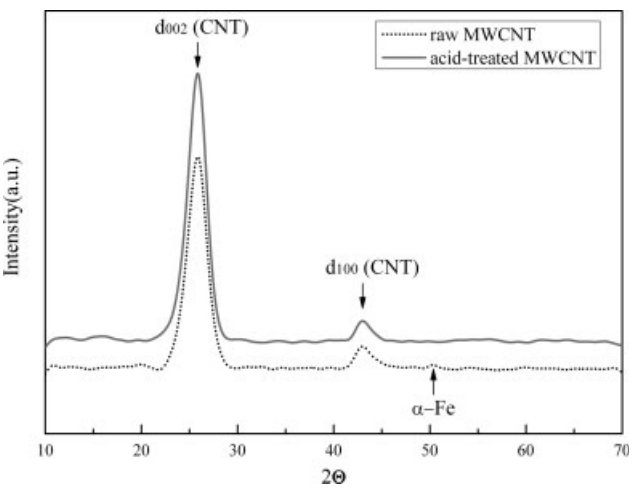

Figure 3 XRD spectra of MWCNTs before and after acid treatment.

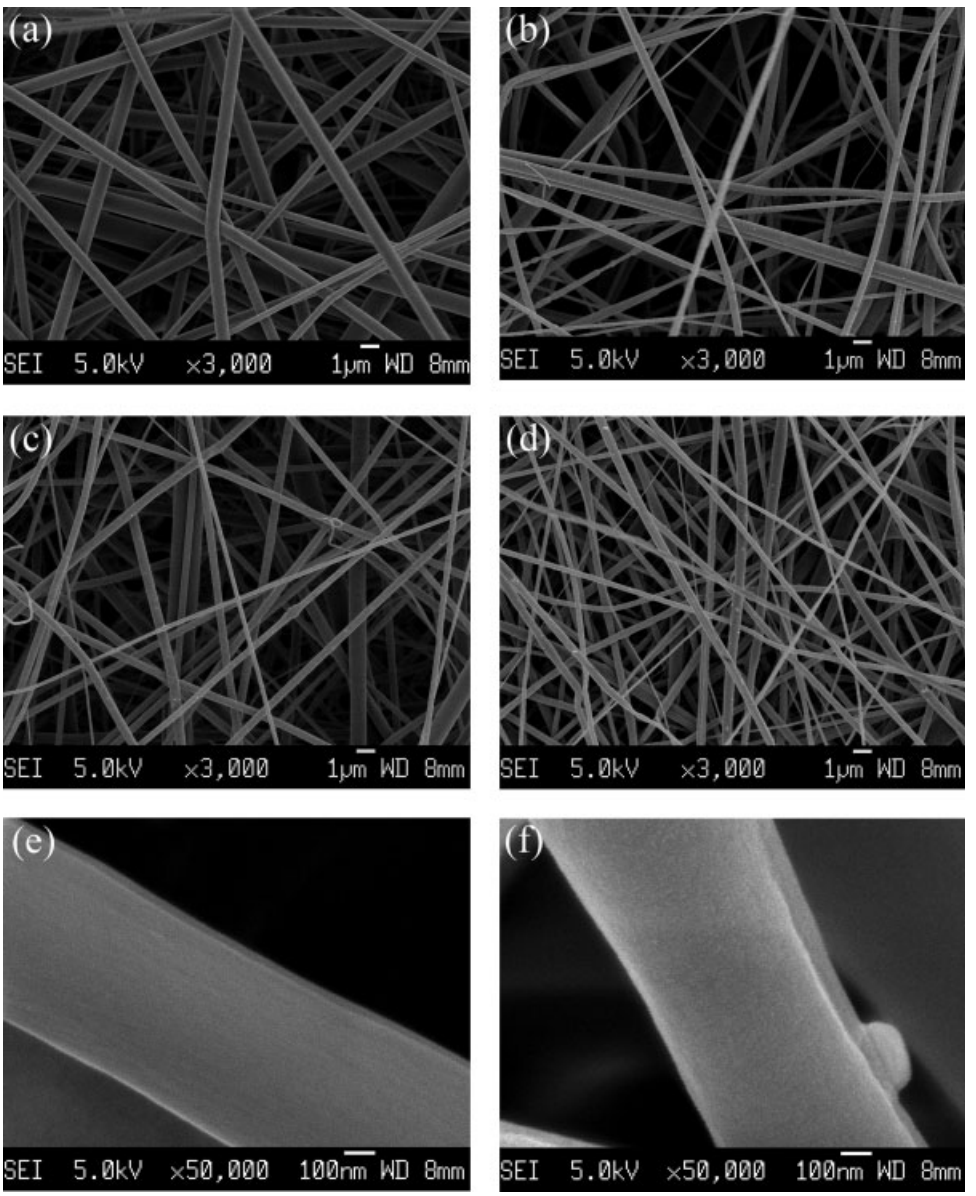

Figure 4 SEM photographs of neat PET and MWCNT/PET nanowebs. (a) neat PET, (b) MWCNT 1 wt %, (c) 2 wt %, (d) 3 wt %, (e) neat PET nanofiber surface, (f) a projection on the surface of PET nanofiber due to curled MWCNTs.

the increase in the diameter of electrospun nanofibers.[33] Dope viscosity increased when MWCNTs were added, but dope viscosity started to decrease as the shear rate became higher (Fig. 5). This shear thinning behavior became more obvious at higher MWCNT concentrations. It is thought that MWCNTs of one-dimensional structure were oriented to some extent at high shearing rate and thus induced the rapid decrease in dope viscosity.[34] But in the case of 3 wt % MWCNT/PET solution, viscosity in the lower shear rate range did not increase and the shear thinning effect became weaker in comparison with 2 wt % MWCNT/PET solution. Occurrence of MWCNT aggregation at high concentration may be responsible for this result.

Electrospinning is a process undertaken at high shear rate ($>10^3$ s^{-1}), thus the increased viscosity effect of MWCNT addition became insignificant due to the shear thinning phenomenon of MWCNTs. Also, the distribution of nanofiber diameters changed with MWCNT concentration. In comparison with neat PET nanoweb, MWCNT/PET nanowebs had relatively thinner nanofibers with diameters of 100 $\sim$ 200 nm. It is thought that the relatively stronger stretch applied to the dope portion including locally aggregated MWCNTs is responsible for this. As shown in Figure 6, high portions of thinner nanofibers were obtained more frequently in nanowebs with higher concentrations of MWCNT. This is because part of the electrospinning solution with

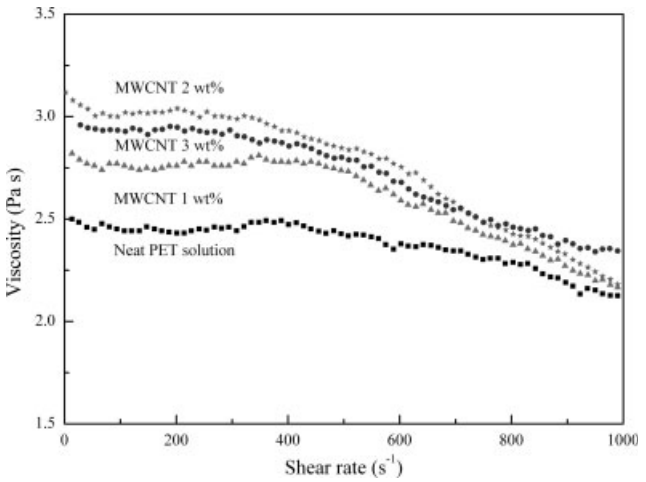

Figure 5 Plot of viscosity versus shear rate for neat PET and MWCNT/PET dope.

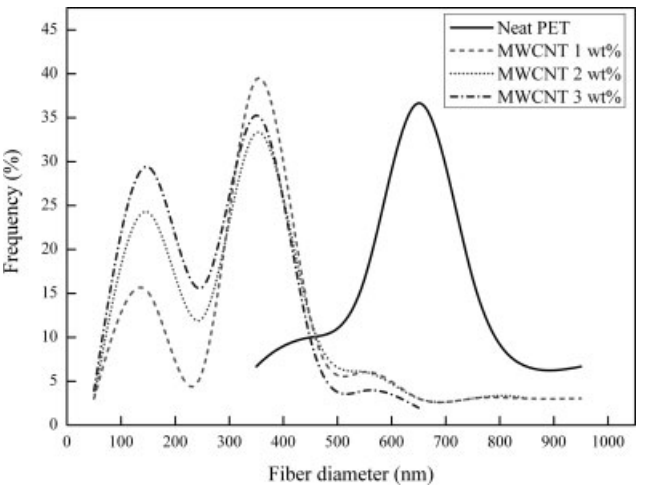

Figure 6 Fiber diameter distributions of neat PET and MWCNT/PET nanofibers.

higher MWCNT concentration will result in thinner nanofibers than the rest of the electrospinning solution. Consequently, the distribution of nanofiber diameters showed a bimodal shape when MWCNT was added.

Figure 7 shows the TEM images of MWCNT/PET nanofibers. At the lower concentration (1 wt %), MWCNTs were well aligned along the nanofiber axis. At the higher concentration (3 wt %), MWCNTs were basically aligned along the nanofiber axis, but the anisotropy decreased. Also some notches due to distorted MWCNTs were observed as shown in SEM photo [Fig. 4(f)]. MWCNTs used here were produced by CVD pyrolysis and thus hydrocarbon structures are not perfect. So, MWCNTs of the bent or helical shapes are shown. It is thought that these curved MWCNTs are easy to make agglomeration during electrospinning and thus anisotropy decreases as the concentration of MWCNTs increase. The length of MWCNTs was shortened comparing to as-received state. The rupture of MWCNTs by acid treatment and sonication process are responsible for it.

Thermal properties

Differential scanning calorimetry result. The differential scanning calorimetry thermograms are shown in Figure 8. The heat of cold crystallization and fusion were obtained from the peak area of DSC thermograms. The degree of crystallinity before and after cold crystallization, χ_{bc} and χ_{ac}, cold crystallization temperature T_{cc} and melting temperature T_m are summarized in Table I. The degree of crystallinity before cold crystallization increased with increasing MWCNT concentration. It is probable that more stretching of the electrospinning dope due to MWCNT addition helped the formation and

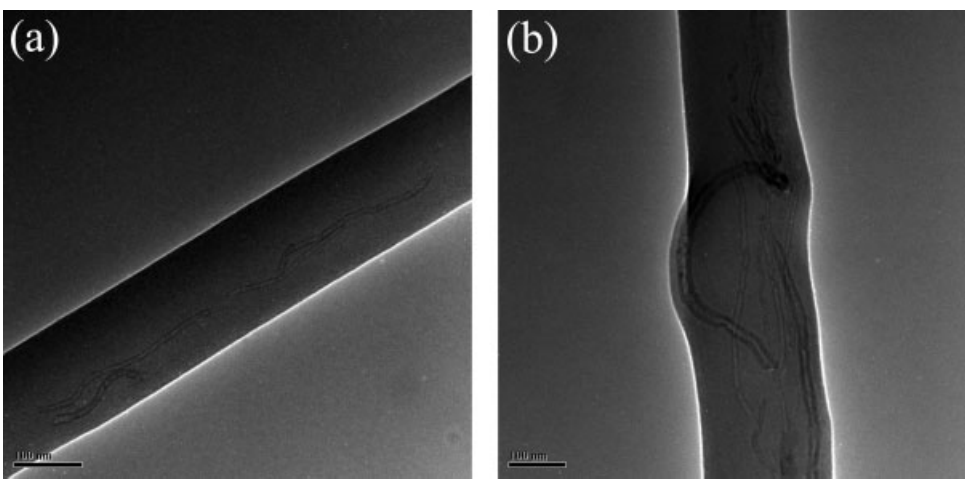

Figure 7 TEM images of MWCNT/PET nanofiber containing of (a) 1 wt % and (b) 3 wt % MWCNT.

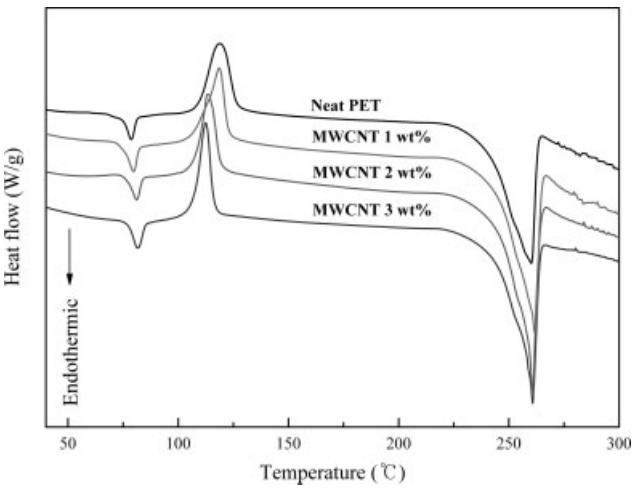

Figure 8 DSC thermograms of neat PET and MWCNT/PET nanowebs.

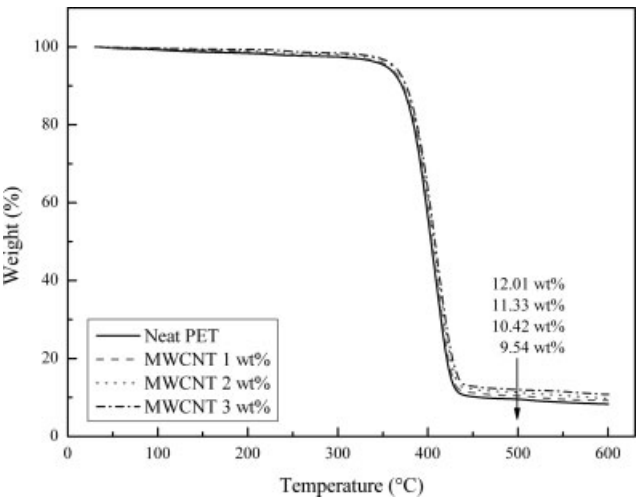

Figure 9 TGA thermograms of neat PET and MWCNT/PET nanowebs.

arrangement of the crystalline. As MWCNT concentration increases, T_{cc} and the onset temperature of cold crystallization moved to a lower temperature and the cold crystallization peak became sharper, indicating that cold crystallization started earlier and duration of crystallization became shorter.

It is known that dispersed CNTs in polymer matrix can act as nucleation agents.[35] Consequently, the cold crystallization of PET can start at lower temperatures and progress faster. After cold crystallization, the degree of crystallinity of all four nanowebs showed similar values regardless of MWCNT concentration, suggesting that increment of the degree of crystallinity by cold crystallization decreased with increasing MWCNT concentration. Cold crystallization is the process of crystal arrangement and formation at the interface between crystalline and amorphous regions. It is thought that though CNTs can act as nucleating agents, overall increment of crystallinity was limited due to the effect of polymer chain confinement by CNT addition. T_m did not change obviously according to the existence of MWCNT. Generally, the crystallinity of electrospun nanowebs was lower than that of conventional PET films or yarns because the electrospinning process does not include the additional annealing process standard for PET films and yarns and the formation of nanofibers is a rapid process, allowing little time for the crystalline region to grow.[36]

Thermogravimetric analysis

Thermal stability of MWCNT/PET nanowebs was investigated by thermogravimetric analysis. Thermograms of samples show that MWCNT/PET nanowebs including higher contents of MWCNTs has better thermal stability (Fig. 9).

The 5, 10 wt % weight loss temperature ($T_{5\ wt\ \%}$, $T_{10\ wt\ \%}$) and residue at 500°C for samples are listed in Table II. It is shown that MWCNT/PET nanoweb with higher concentration of MWCNT has a higher $T_{5\ wt\ \%}$ and $T_{10\ wt\ \%}$, and the increment of $T_{5\ wt\ \%}$ and $T_{10\ wt\ \%}$ becomes larger with increasing MWCNT concentration upon the whole. Residue at 500°C of neat PET nanoweb was 9.54 wt % and MWCNT/PET nanowebs had a little more residues at 500°C. This difference of residues should be originated from not decomposed MWCNTs. Enhanced thermal stability of electrospun nanowebs by the addition of CNTs was reported in several literatures.[37,38] It is thought that the interfacial interaction between functionalized MWCNTs and PET created by secondary bondings such as Van der Waals or hydrogen bonding retarded the thermal decomposition of PET into cyclic oligomers.[39]

TABLE I
DSC Results of Neat PET and MWCNT/PET Nanowebs

MWCNT conc.(wt %)	T_{cc}(°C)	T_m(°C)	χ_{bc} (%)	χ_{ac} (%)
0	118.8	259.7	13.94	22.74
1	118.5	261.5	14.57	22.87
2	113.5	260.5	15.14	21.98
3	112.2	260.6	16.34	22.23

TABLE II
TGA Results of Neat PET and MWCNT/PET Nanowebs

MWCNT conc. (wt %)	$T_{5\ wt\ \%}$	$T_{10\ wt\ \%}$	Residue at 500°C (wt %)
0	353.4	372.1	9.54
1	356.3	373.4	10.42
2	361.1	376.2	11.33
3	363.1	382.9	12.01

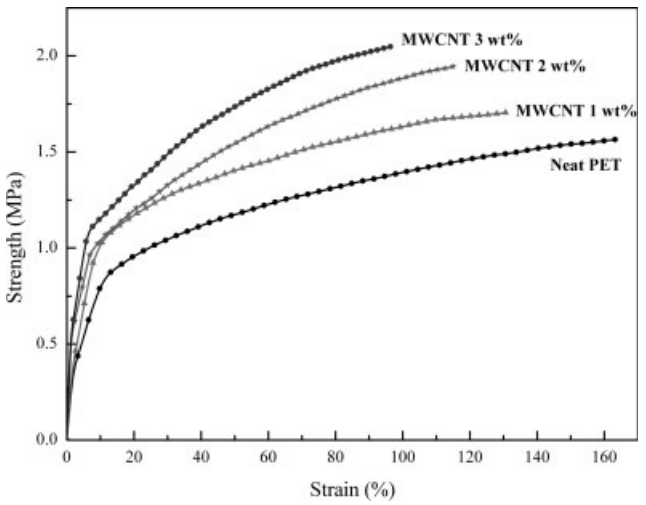

Figure 10 Stress-strain curves of neat PET and MWCNT/PET nanowebs.

Tensile properties

Stress-strain curves

Stress-strain curves of neat PET and MWCNT/PET nanowebs are shown in Figure 10. The tensile strength of neat PET nanoweb was over 10 times lower than that of general PET films or fibers. Absence of postprocessing such as annealing, weak bonding at nanofiber crossovers and the porous structure are responsible for the low tensile strength of nanowebs. The tensile strength increased with increasing MWCNT concentration. Upon 3 wt % MWCNT addition, the tensile strength and modulus were increased by 31.4 and 100.2%, respectively. As MWCNT content increasing, enhancing effect of the tensile strength and modulus was decreased. It is thought that decreasing anisotropy of MWCNTs is responsible for that. This stiffening effect is thought to be induced by three factors: (1) Enhanced crystallinity due to MWCNT addition, (2) Chemical interaction between PET and the carboxyl groups of MWCNTs, (3) Secondary interaction such as Van der Waals bonding between PET and MWCNTs.[40]

According to Ko's work,[41] CNTs hinder the crazing extension of nanofibers because both the alignment of CNTs in the crazing area and the slippage between CNTs consume extra energy. Distribution of CNTs in the polymer matrix and surface interaction between CNTs and the polymer are also important factors determining the reinforcement effect of CNTs in the nanoweb. Greater enhancement of tensile modulus was observed compared to tensile strength. This indicates that the reinforcement effect of MWCNTs is more prominent in the initial tensile region than the postyield region. Elongation at break decreased from 163 to 96% as MWCNT concentration reached 3 wt %, because dispersed MWCNTs hindered the movement of polymer chains. The tensile test results are listed in Table III.

Dynamic mechanical analysis

Figure 11 shows dynamic mechanical analysis results of MWCNT/PET nanowebs. Storage modulus of the nanowebs increased with the increase in MWCNT concentration. These results are consistent with the tensile test results. The difference in storage modulus among the nanowebs was maintained almost constantly before the onset temperature of glass transition. But after the glass transition, there were not large difference among the values of storage modulus. So that, the enhancement of storage modulus by the stiffening effect of MWCNTs is particularly significant before glass transition.

Tan δ peak shifted slightly to the higher temperature region with increased MWCNT concentration, indicating that the glass transition temperature was raised. This result is consistent with the T_g points of DSC thermograms showed in Figure 7. It is thought that MWCNTs hinder the segmental motion of PET chains, thus, increasing of T_g. Also, tan δ peak values decreased with increasing MWCNT concentration. This result suggests that energy loss decreased in nanowebs with higher concentration of MWCNTs, due to enhanced crystallinity as well as MWCNT confinement effect.

Electrical conductivity

The measured electrical conductivity data are listed in Table IV. By the presence of MWCNTs in PET

TABLE III
Tensile Properties of Neat PET and MWCNT/PET Nanowebs

MWCNT conc. (wt %)	Tensile strength (MPa)	Impro. (%)	Tensile modulus (MPa)	Impro. (%)	Elongation at break (%)
0	1.56		10.8		163
		8.9		38.8	
1	1.70		15.0		130
		24.4		89.8	
2	1.94		20.5		115
		31.4		100.2	
3	2.05		21.8		96

nanofibers, electrical conductivity was enhanced up to 4 orders of magnitude. In comparison with CNT nanocomposites or films, the nanowebs have lower electrical conductivity. Electrospun nanowebs have a porous structure, thus there are less channels for electrical conduction than other continuous matrices. Enhancement of the electrical conductivity of nanocomposites by fillers is influenced by not only the degree of filler dispersion in the matrix but also the filler configuration. For example, MWCNT/nylon 6 nanowebs obtained by adsorbing MWCNTs onto the surface of nylon 6 nanofibers showed high electrical conductivity (0.15 S/cm) with 1.5 wt % of MWCNTs.[42] On the contrary, SWCNT/nylon 6,6 nanocomposite obtained using the melt extruder showed electrical conductivity of five-order lower value at the same CNT concentration.[43] In the viewpoint of filler continuance, nanowebs with MWCNTs concentrated on the surface of the nanofibers are more advantageous for electrical conduction than nanoweb with MWCNTs dispersed in the polymer matrix. Our MWCNT/PET nanowebs showed relatively lower values of electrical conductivity because MWCNTs dispersed in PET nanofibers do not necessarily construct a continuous channel of electrical conduction.

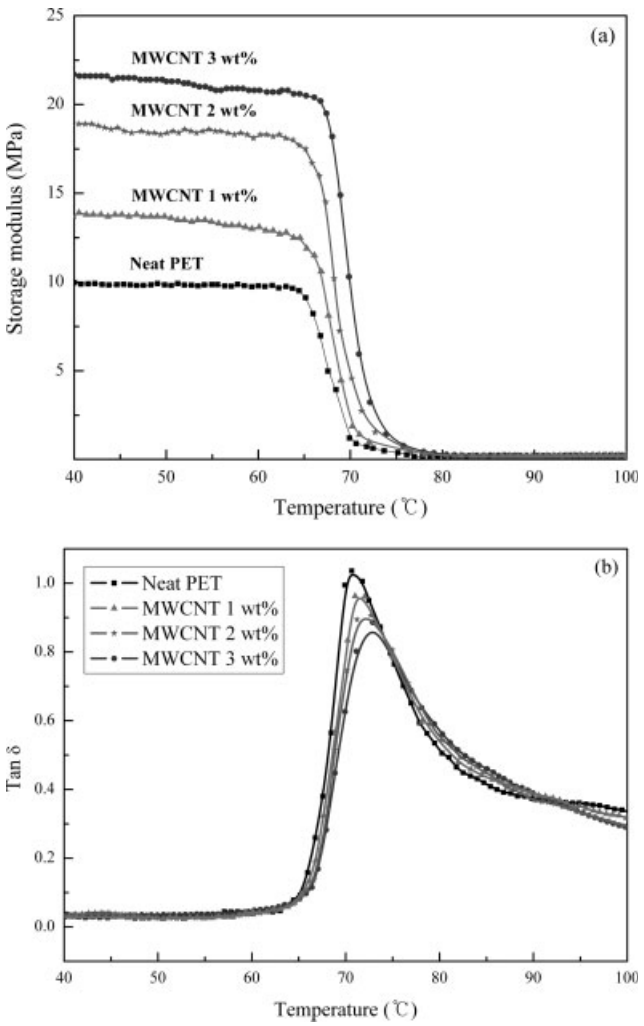

Figure 11 Dynamic mechanical analysis results of neat PET and MWCNT/PET nanowebs. (a) Storage moduli and (b) tan δ curves.

TABLE IV
Electrical Conductivities of Neat PET and MWCNT/PET Nanowebs

MWCNT conc. (wt %)	Electrical conductivity (S/cm)
0	6.25×10^{-12}
1	2.35×10^{-9}
2	7.48×10^{-9}
3	4.05×10^{-8}

CONCLUSIONS

Functionalized MWCNTs were prepared by acid treatment, and MWCNT/PET nanowebs were fabricated using electrospinning. Introduction of carboxyl groups onto the surface of MWCNTs and removal of any metal residuals were confirmed by FTIR and XRD analysis. By MWCNTs acting as charge carriers and their shear thinning effect, the diameter of nanofibers decreased with increasing MWCNT concentration. The addition of MWCNT produced a bimodal nanofiber diameter distribution curve because of the presence of locally aggregated MWCNTs. DSC results showed that the degree of crystallinity was increased by MWCNT addition. Because of the enhanced crystallinity and interaction between MWCNTs and PET, tensile strength, and modulus of MWCNT/PET nanowebs were increased. At 3 wt % MWCNT concentration, tensile strength and modulus were enhanced by 31.4 and 100.2%, respectively. Dynamic mechanical analysis showed consistent results with the tensile test. Thermogravimetric analysis showed that thermal stability was increased by MWCNT addition. Electrical conductivity was increased by MWCNT addition, and the enhanced values ($\sim 10^{-8}$ S/cm) were in the acceptable range for electrostatic dissipation. MWCNT/PET nanowebs with their enhanced mechanical and thermal properties, high porosity and flexibility, and electrical conductivity of antistatic level, could be used in high performance air filtration applications or membrane material having electrostatic dissipation.

References

1. Iijima, S. Nature 1991, 354, 56.
2. Treacy, M. M. J.; Ebbesen, T. W.; Gibson, J. M. Nature 1996, 381, 678.
3. Dai, H.; Wong, E. W.; Lieber, C. M. Science 1996, 272, 523.

4. Tombler, T.; Zhou, C.; Alexseyev, L.; Kong, J.; Dai, H.; Liu, L.; Jayanthi, C. S.; Tang, M.; Wu, S. Nature 2000, 405, 769.
5. De Pablo, P. J.; Martinez, M. T.; Colchero, J.; Gomez-Herrero, J.; Maser, W. K.; De Benito, A. M.; Munoz, E.; Baro, A. M. Mater Sci Eng C 2001, 15, 149.
6. Li, X.; Huang, Y. D.; Liu, L.; Cao, H. L. J Appl Polym Sci 2006, 102, 2500.
7. Valentini, L.; Biagiotti, J.; Kenny, J. M.; López Manchado, M. A. J Appl Polym Sci 2003, 89, 2657.
8. Safadi, B.; Andrews, R.; Grulke, E. A. J Appl Polym Sci 2002, 84, 2660.
9. Shin, D. H.; Yoon, K. H.; Kwon, O. H.; Min, B. G.; Hwang, C. I. J Appl Polym Sci 2006, 99, 900.
10. Hou, H.; Ge, J. J.; Zeng, J.; Li, Q.; Reneker, D. H.; Greiner, A.; Chen, S. Z. D. Chem Mater 2005, 17, 967.
11. Hou, H.; Reneker, D. H. Adv Mater 2004, 16, 69.
12. Coffin, D. W.; Carlsson, L. A.; Pipes, R. B. Compos Sci Technol 2006, 66, 1132.
13. Ding, W.; Eitan, A.; Fisher, F. T.; Chen, X.; Dikin, D. A.; Andrews, R.; Brinson, L. C.; Schadler, L. S.; Ruoff, R. S. Nano Lett 2003, 3, 1593.
14. Gong, X.; Liu, J.; Baskaran, S.; Voise, R. D.; Young, J. S. Chem Mater 2000, 12, 1049.
15. Liu, P. Eur Polym Mater 2005, 41, 2693.
16. Feng, L.; Li, S.; Li, H.; Zhai, J.; Song, Y.; Jiang, L.; Zhu, D. Angew Chem Int Ed 2002, 41, 1221.
17. Ma, P. X.; Zhang, R. J Biomed Mat Res 1999, 46, 60.
18. Liu, G. J.; Ding, J. F.; Qiao, L. J.; Guo, A.; Dymov, B. P.; Gleeson, J. T.; Hashimoto, T.; Saijo, K. Chem Eur J 1999, 5, 2740.
19. Reneker, D. H.; Chun, I. S. Nanotechnol 1996, 7, 216.
20. Deitzel, J. M.; Kleinmeyer, J. D.; Hirvonen, J. K.; Beck Tan, N. C. Polymer 2001, 42, 8163.
21. Huang, Z. M.; Zhang, Y. Z.; Kotaki, M.; Ramakrishna, S. Compos Sci Technol 2003, 63, 2223.
22. Gupta, P.; Asmatulu, R.; Claus, R.; Wilkes, G. J Appl Polym Sci 2006, 100, 4935.
23. Hong, K. H.; Kang, T. J. J Appl Polym Sci 2006, 99, 1277.
24. Ayutsede, J.; Gandhi, M.; Sukigara, S.; Ye, H.; Hsu, C.; Gogotsi, Y.; Ko, F. Biomacromolecules 2006, 7, 208.
25. Tzavalas, S.; Gregoriou, V. G. Vib Spectrosc 2008, 46, 135.
26. Li, J.; Gao, X.; Tong, Y. Synth Fiber Ind 2004, 27, 16.
27. Li, Z.; Luo, G.; Wei, F.; Huang, Y. Compos Sci Technol 2006, 66, 1022.
28. Hong, K. H.; Oh, K. W.; Kang, T. J. J Appl Polym Sci 2005, 96, 983.
29. Shaffer, M. S. P.; Fan, X.; Windle, A. H. Carbon 1998, 36, 1603.
30. Zhou, O.; Fleming, R. M.; Murphy, D. W.; Chen, C. H.; Haddon, R. C.; Ramirez, A. P.; Glarum, S. H. Science 1994, 263, 1744.
31. Müller, C.; Golberg, D.; Leonhardt, A.; Hampel, S.; Büchner, B. Phys Status Solidi A 2006, 203, 1064.
32. Shin, Y. M.; Hohman, M. M.; Brenner, M. P.; Rutledge, G. C. Appl Phys Lett 2001, 178, 1149.
33. McKee, M. G.; Wilkes, G. L.; Colby, R. H.; Long T. E. Macromolecules 2004, 37, 1760.
34. Hwang, S. H.; Paeng, S. W.; Kim, J. Y.; Huh, W. Polym Bull 2003, 49, 329.
35. Sandler, J.; Broza, G.; Nolte, M.; Schulte, K.; Lam, Y. M.; Shaffer, M. S. J Macromol Sci B 2003, 42, 479.
36. Li, Y.; Huang, Z. M.; Lu, Y. Eur Polym Mater 2006, 42, 1696.
37. Ge, J. J.; Hou, H.; Li, Q.; Graham, M. J.; Greiner, A.; Reneker, D. H.; Harris, F. W.; Stephen, Z. D.; Cheng, J. Am Chem Soc 2004, 126, 15754.
38. Mathew, G.; Hong, J. P.; Rhee, J. M.; Lee, H. S.; Nah, C. Polym Test 2005, 24, 712.
39. Samperi, F.; Puglisi, C.; Alicata, R.; Montaudo, G. Polym Degrad Stab 2004, 83, 3.
40. Schadler, L. S.; Giannaris, S. C.; Ajayan, P. M. Appl Phys Lett 1998, 73, 3842.
41. Ye, H.; Lam, H.; Titchenal, N.; Gogotsi, Y.; Ko, F. Appl Phys Lett 2004, 85, 1775.
42. Kim, H. S.; Jin, H. J.; Myung, S. J.; Kang, M. S.; Chin, I. J Macromol Rapid Commun 2006, 27, 146.
43. Haggenmueller, R.; Du, F.; Fischer, J. E.; Winey, K. I. Polymer 2006, 47, 2381.